EUROPEAN ORGANIZATION FOR NUCLEAR RESEARCH

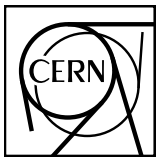

ALICE-ANA-2014-xxx
August 13, 2015

Baryon-antibaryon ($p\bar{p}$, $p\bar{\Lambda}$, $\bar{p}\Lambda$) femtoscopic correlations in Pb–Pb collisions at $\sqrt{s_{\mathrm{NN}}} = 2.76$ TeV

Dominik Aromiński[1], Adam Kisiel[1], Maciej Szymański[1]

1. Warsaw University of Technology

Email: maszyman@cern.ch

Abstract

Here goes your abstract

1 Introduction

In the analysis, we present the measurements of baryon-antibaryon correlations in Pb–Pb collisions at $\sqrt{s_{\mathrm{NN}}} = 2.76$ TeV registered by the ALICE experiment. The method of two-particle correlations (commonly referred to as *femtoscopy*) allows for extracting the space-time characteristics of the emitting source created in heavy-ion collision. Using this technique one can also attempt to extract paramters of strong interaction [1].

2 Data analysis

2.1 Data sample

2.1.1 Data selection

2.1.2 Monte Carlo

2.2 Event selection

2.3 Particle identification

QA plots needed

2.3.1 (Anti-)protons identification

2.3.2 (Anti-)lambdas identification

2.4 Track selection

2.5 Pair selection

2.6 Proton and lambda fraction with respect to their origin

In order to estimate fraction of protons and lambdas coming from certain parent particles was calculated using Monte Carlo Hijing LHC12a17afix. Fractions were checked before reconstruction (pure Monte Carlo) as well as after Geant simulation. Kinematic cuts were applied with the same values as in collision data. It was noticed that before reconstruction, there is a significant contribution of protons at low p_T with PDG of mothers corresponding to π, K^0_L, K^0_S, K^+, D^+_S, J/ψ, B^0, B^+, B^0_S which presumably come from interactions with material. Results were also cross checked with Therminator2 simulation without reconstruction stage. Results are show in Fig. **??**

DCA cut ?!

3 Results

3.1 Correlation functions

3.1.1 Comparison of magnetic field orientations

3.1.2 Non-femtoscopic background

3.1.3 Event plane selection method

3.1.4 Correlation function from Monte Carlo

3.2 Fitting procedure

3.2.1 Residual correlations

3.2.2 $\mathrm{p\bar{p}}$ *theoretical function*

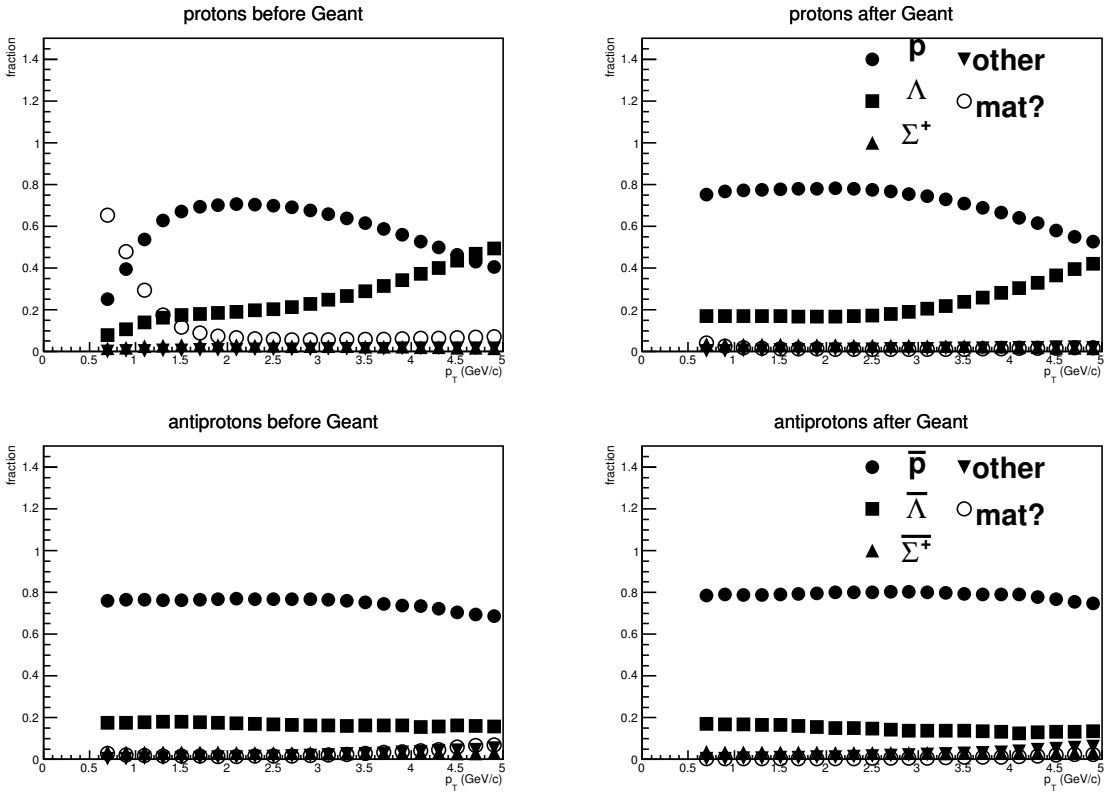

Fig. 1: Hijing p fraction

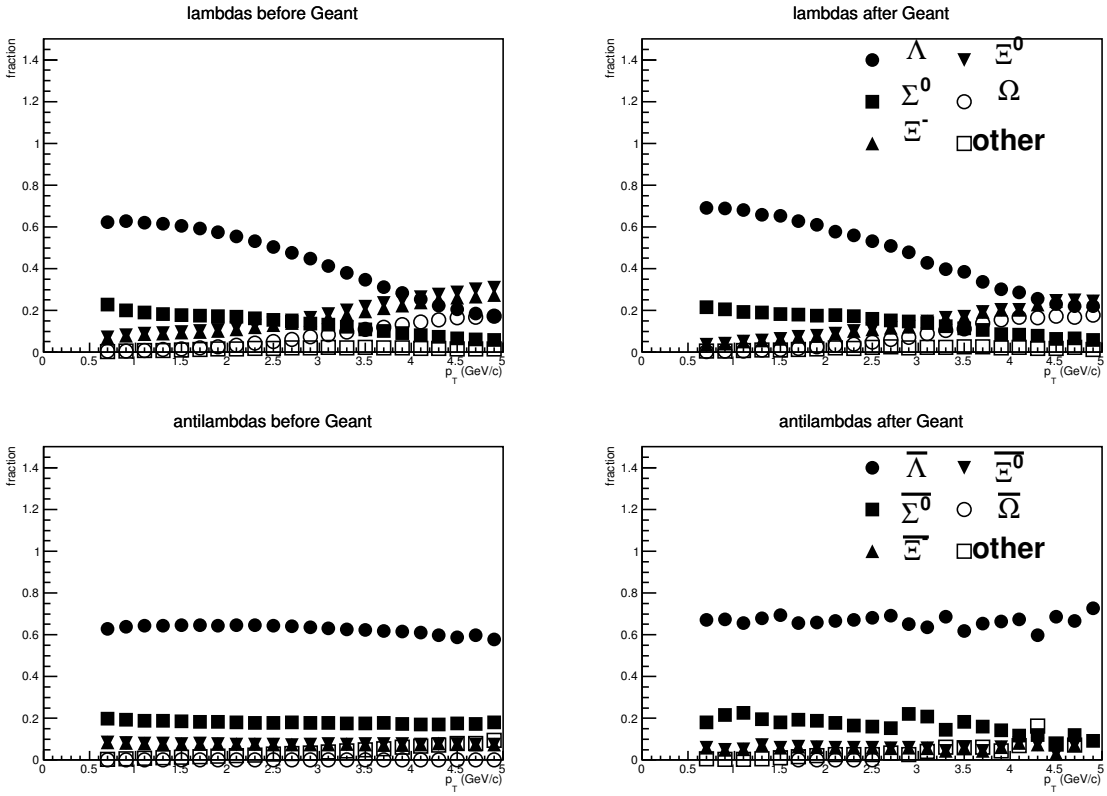

Fig. 2: Hijing Λ fraction

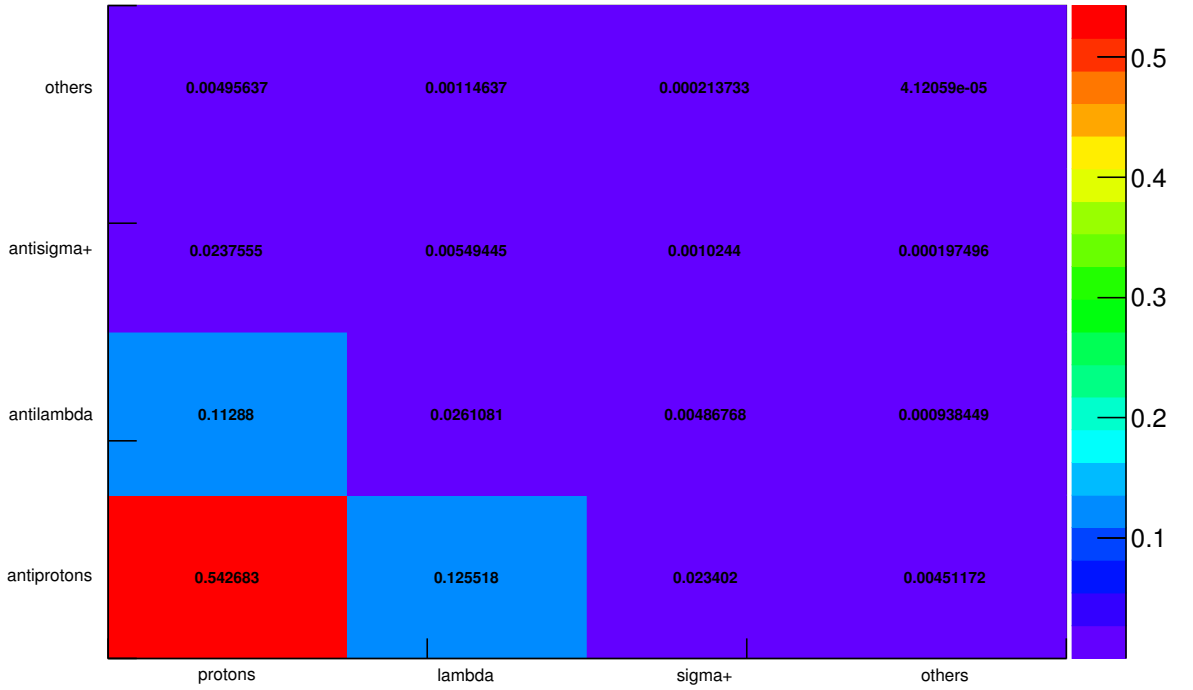

Fig. 3: Hijing+Geant $\mathrm{p\bar{p}}$ Fraction p_T integrated, taking into account 0.95 p and $\bar{\mathrm{p}}$ PID purity

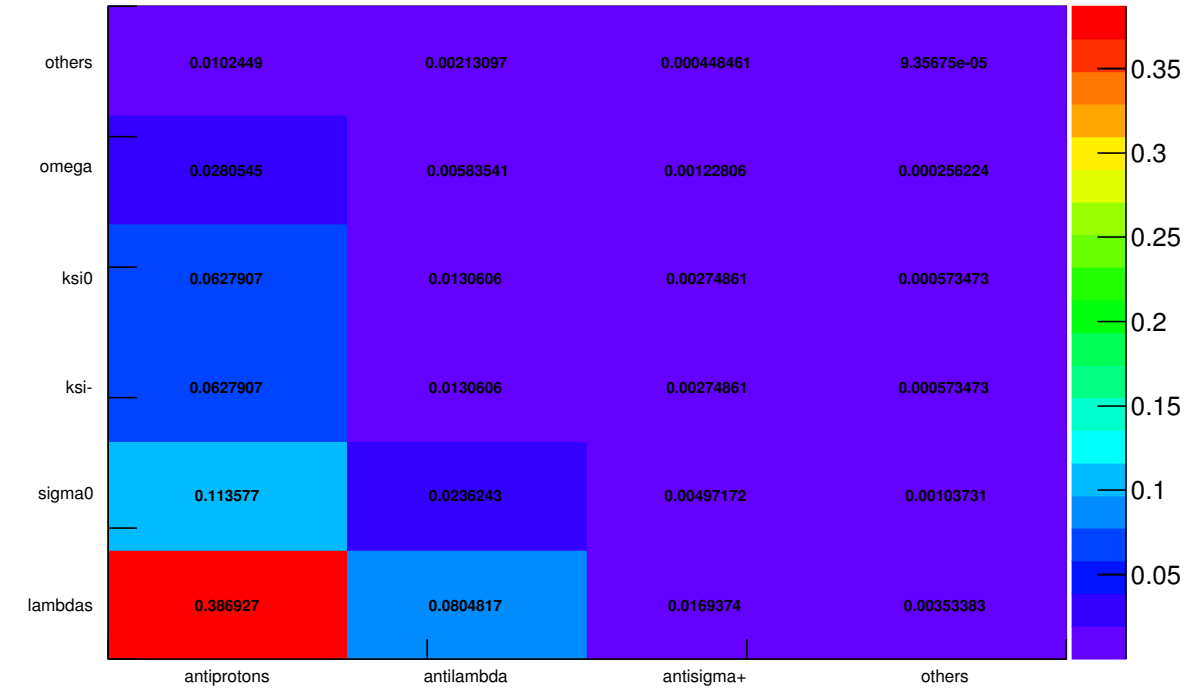

Fig. 4: Hijing+Geant $\bar{\mathrm{p}}\Lambda$ Fraction p_T integrated, taking into account 0.95 $\bar{\mathrm{p}}$ PID purity and 0.9 Λ purity

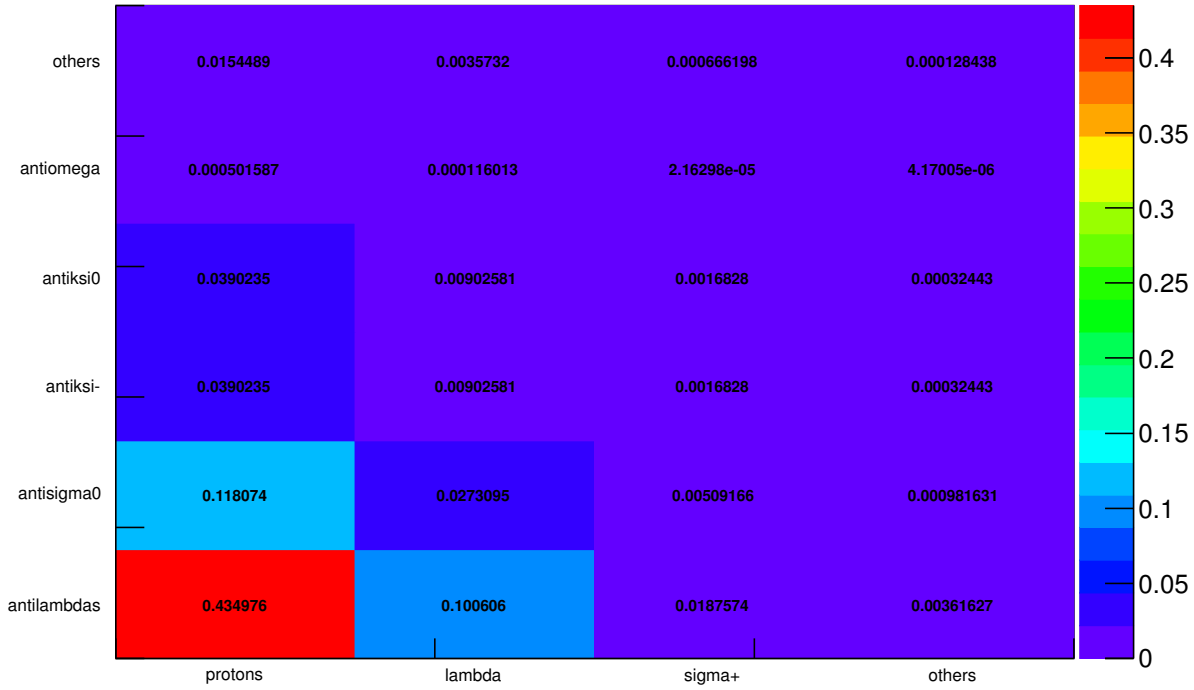

Fig. 5: Hijing+Geant p$\bar{\Lambda}$ Fraction p_T integrated, 0.95 p PID purity and 0.9 $\bar{\Lambda}$ purity

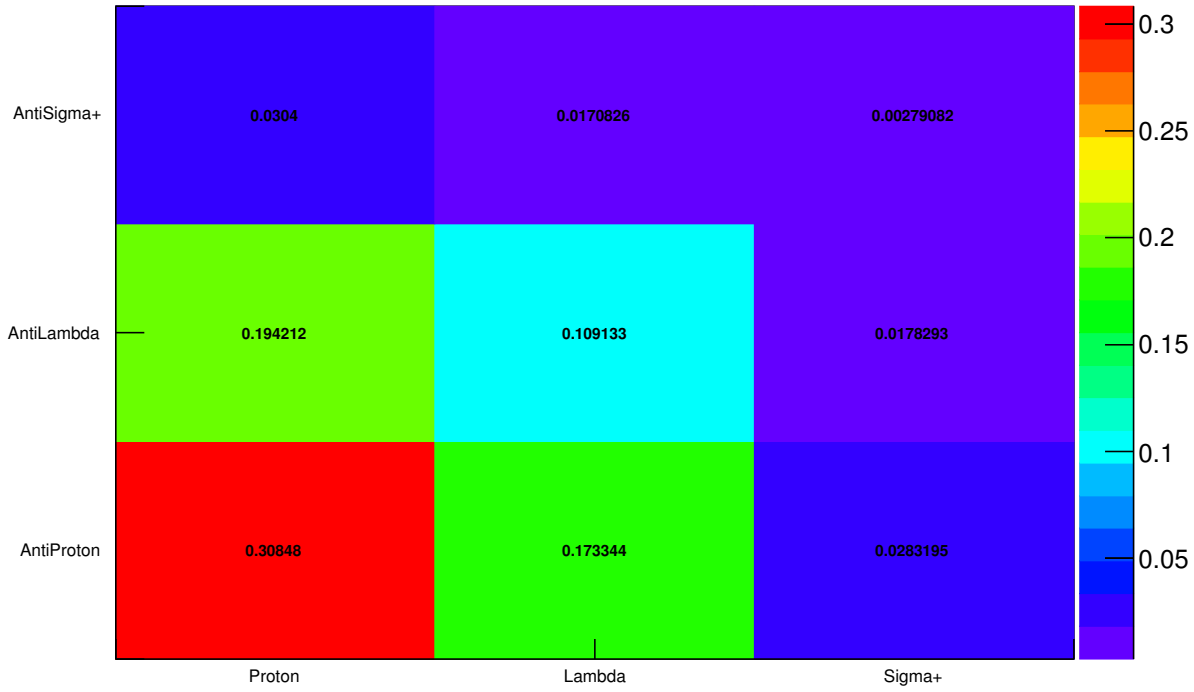

Fig. 6: Therminator2 p$\bar{\text{p}}$ fraction

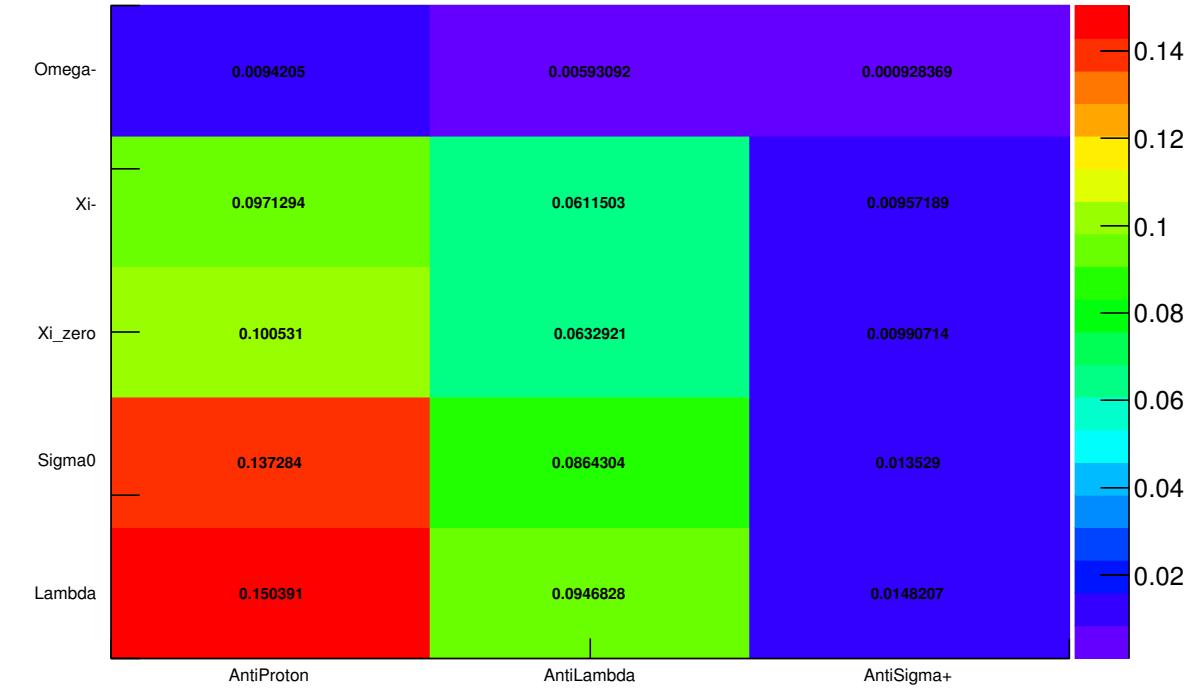

Fig. 7: Therminator2 $\bar{\text{p}}\Lambda$ fraction

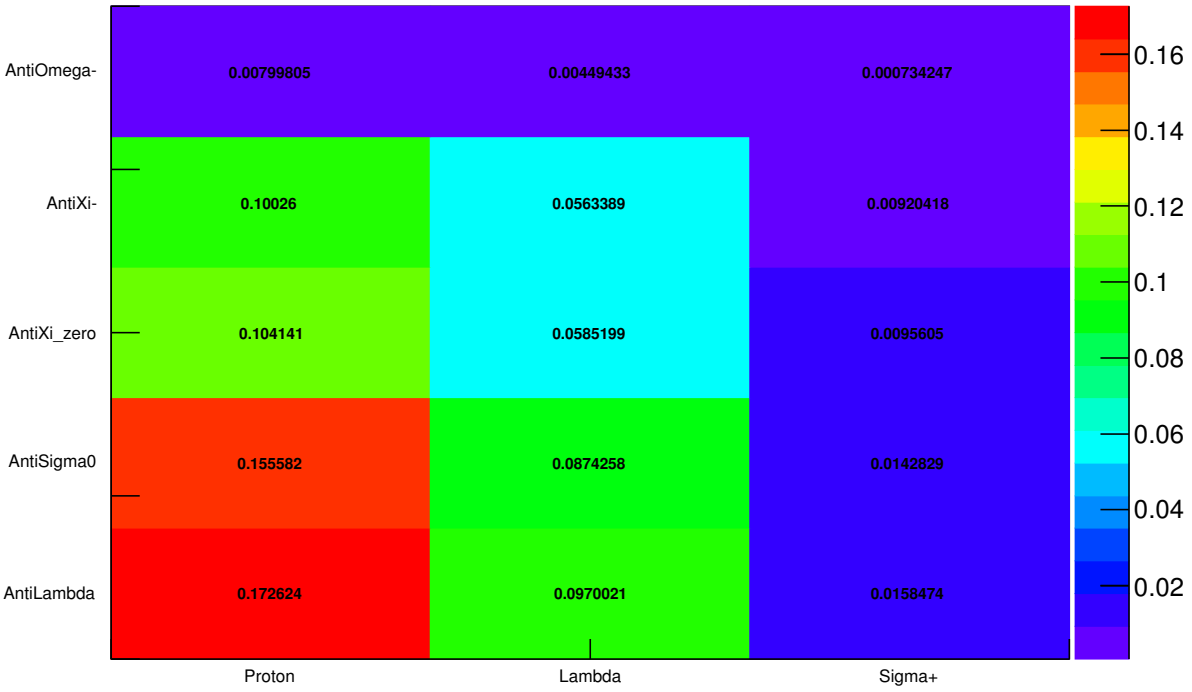

Fig. 8: Therminator2 $\text{p}\bar{\Lambda}$ fraction

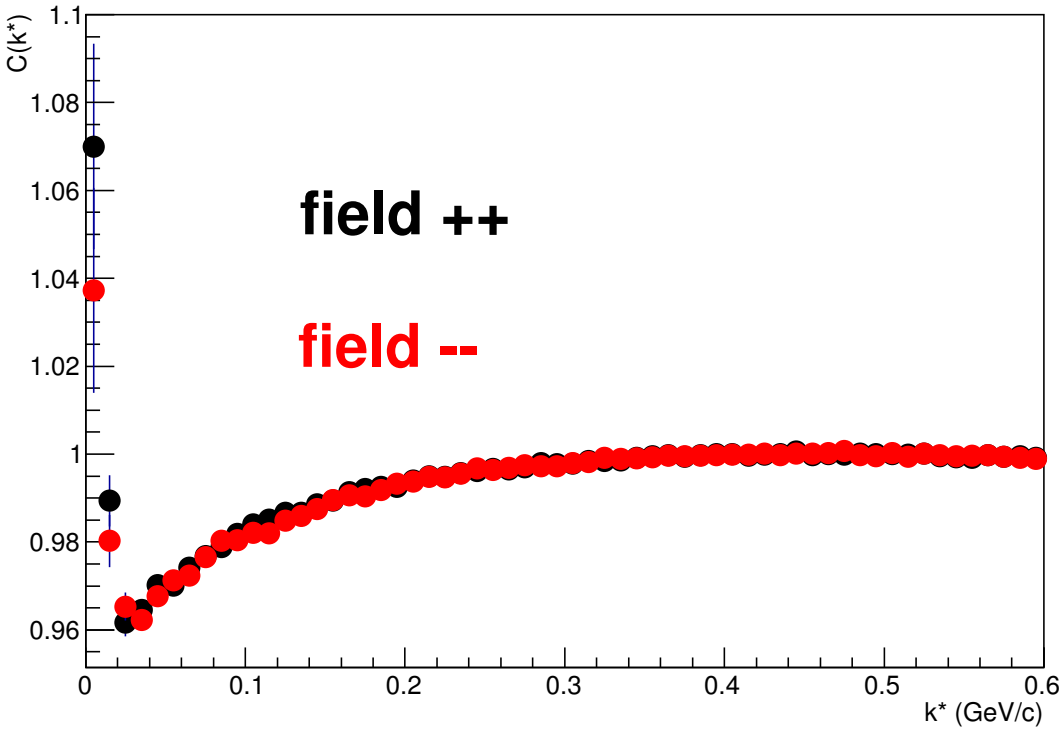

Fig. 9: $p\bar{p}$ correlation function, centrality 0-10%, magnetic field comparison

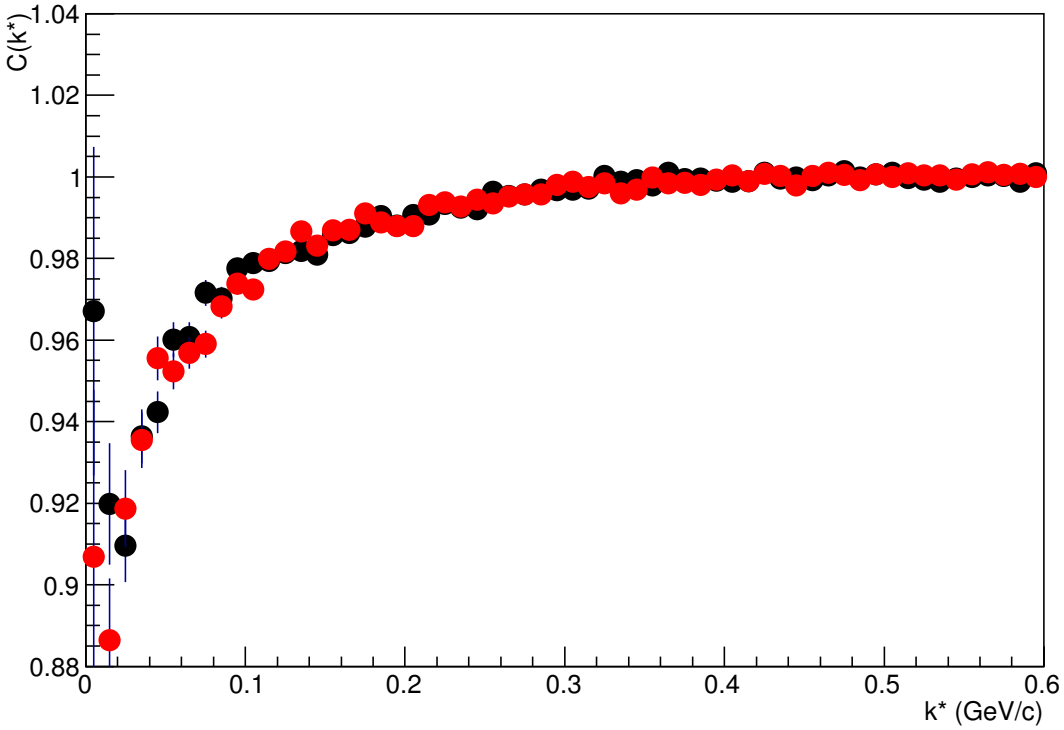

Fig. 10: $p\bar{\Lambda}$ correlation function, centrality 0-10%, magnetic field comparison

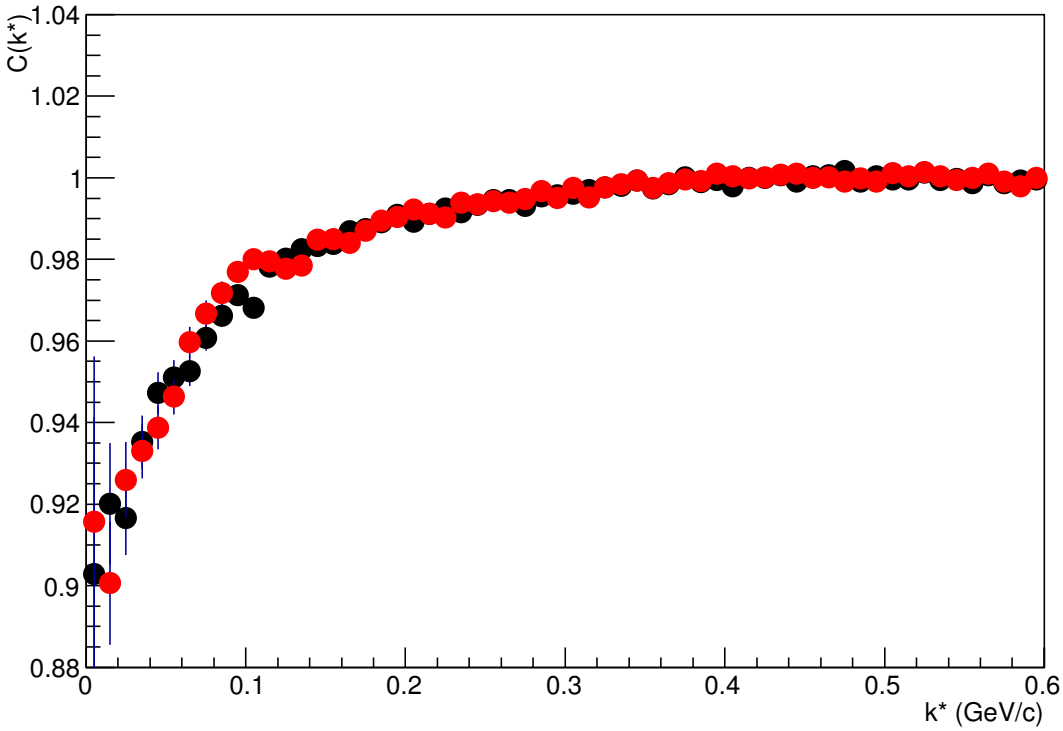

Fig. 11: $\bar{p}\Lambda$ correlation function, centrality 0-10%, magnetic field comparison

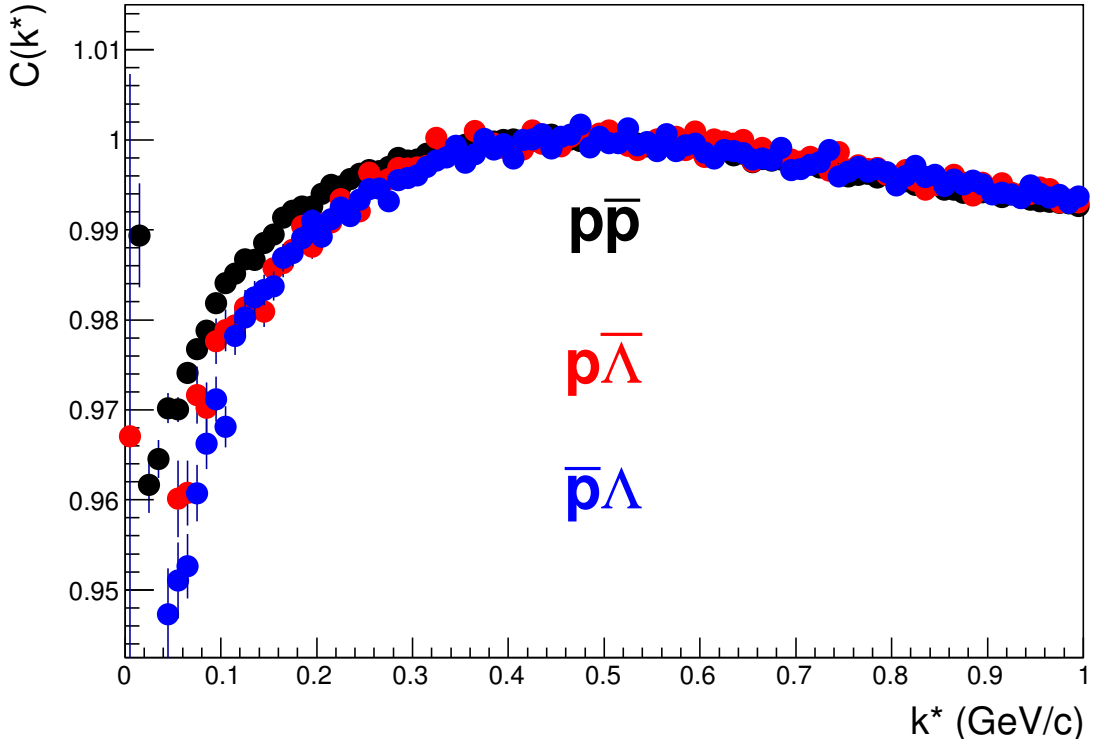

Fig. 12: Non-femtoscopic background in $p\bar{p}$, $p\bar{\Lambda}$, $\bar{p}\Lambda$, centrality 0-10%

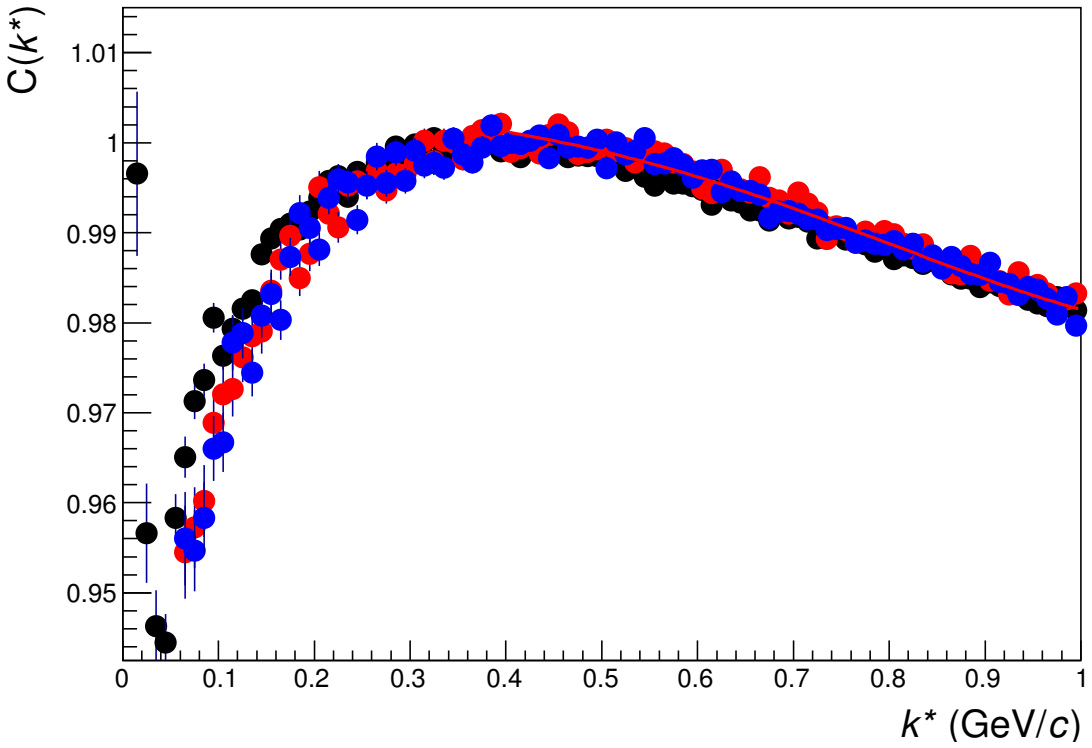

Fig. 13: Non-femtoscopic background in $p\bar{p}$, $p\bar{\Lambda}$, $\bar{p}\Lambda$, centrality 10-30%

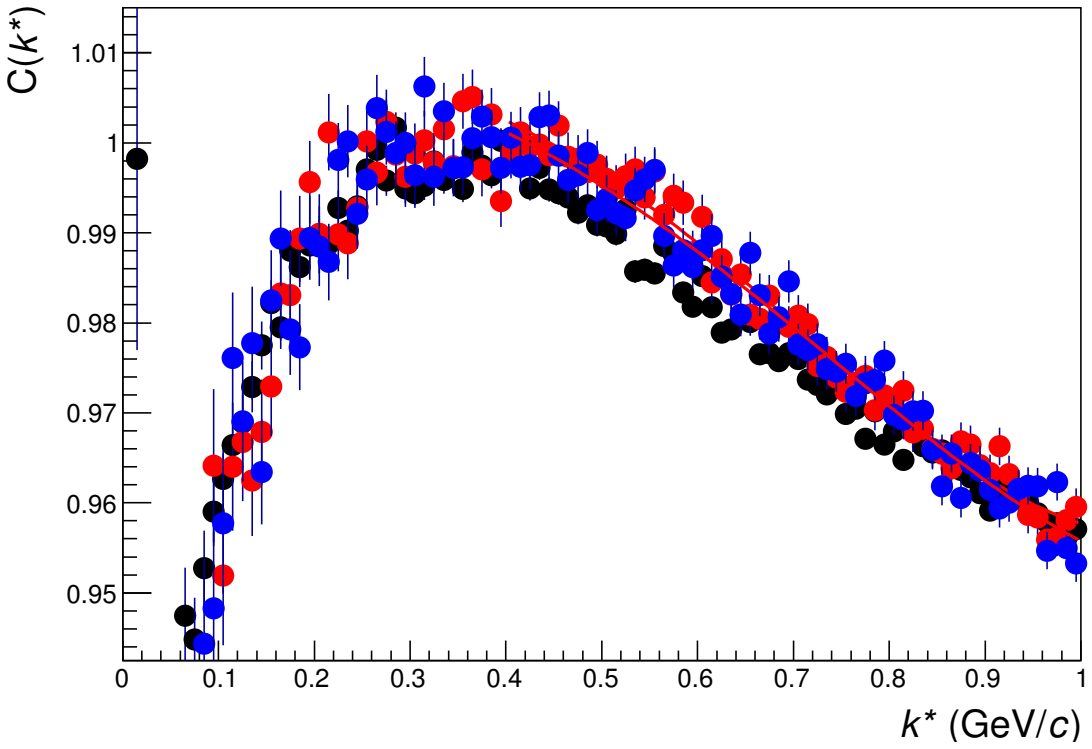

Fig. 14: Non-femtoscopic background in $p\bar{p}$, $p\bar{\Lambda}$, $\bar{p}\Lambda$, centrality 30-50%

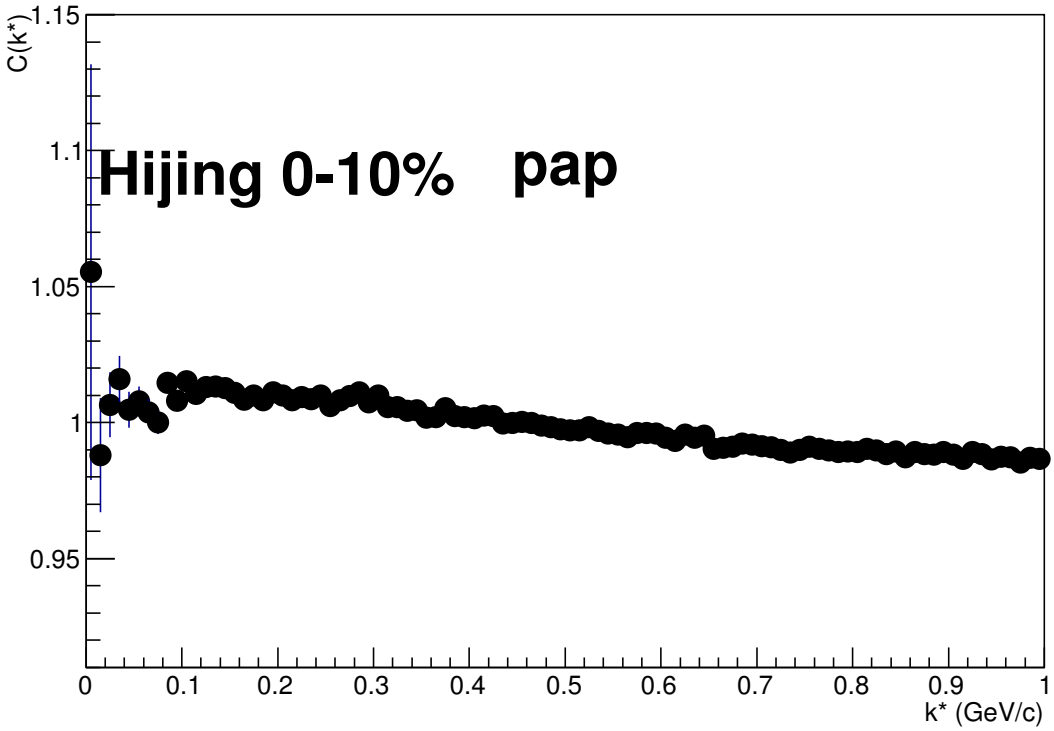

Fig. 15: $p\bar{p}$ correlation function, centrality 0-10%, hijing

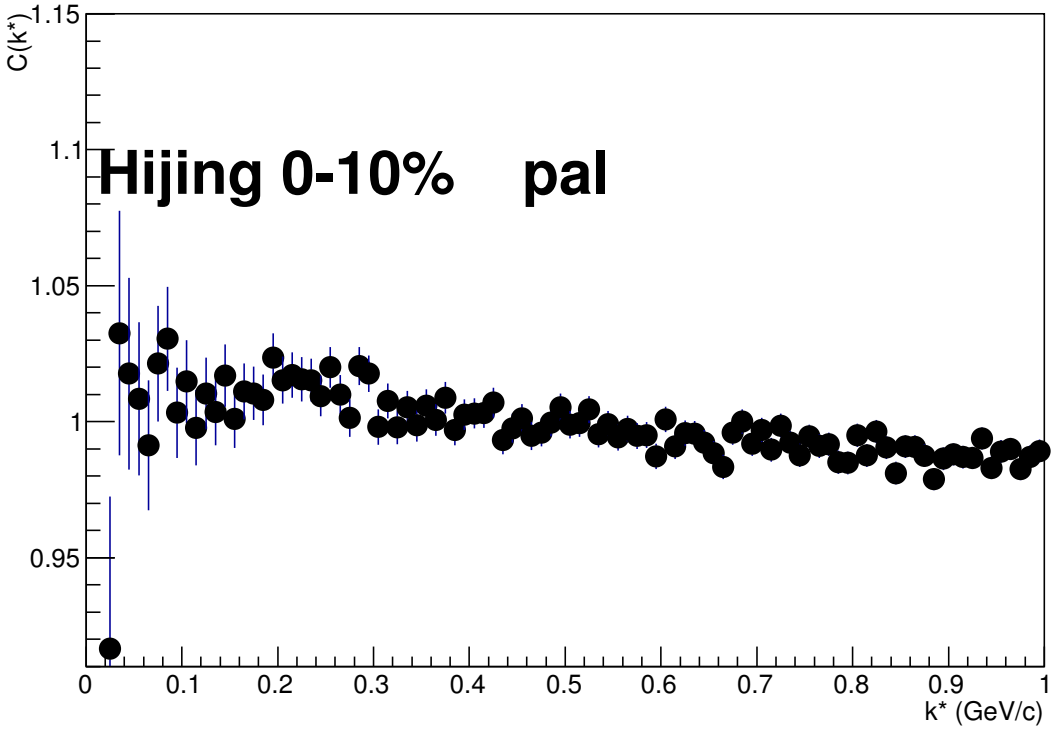

Fig. 16: $p\bar{\Lambda}$ correlation function, centrality 0-10%, hijing

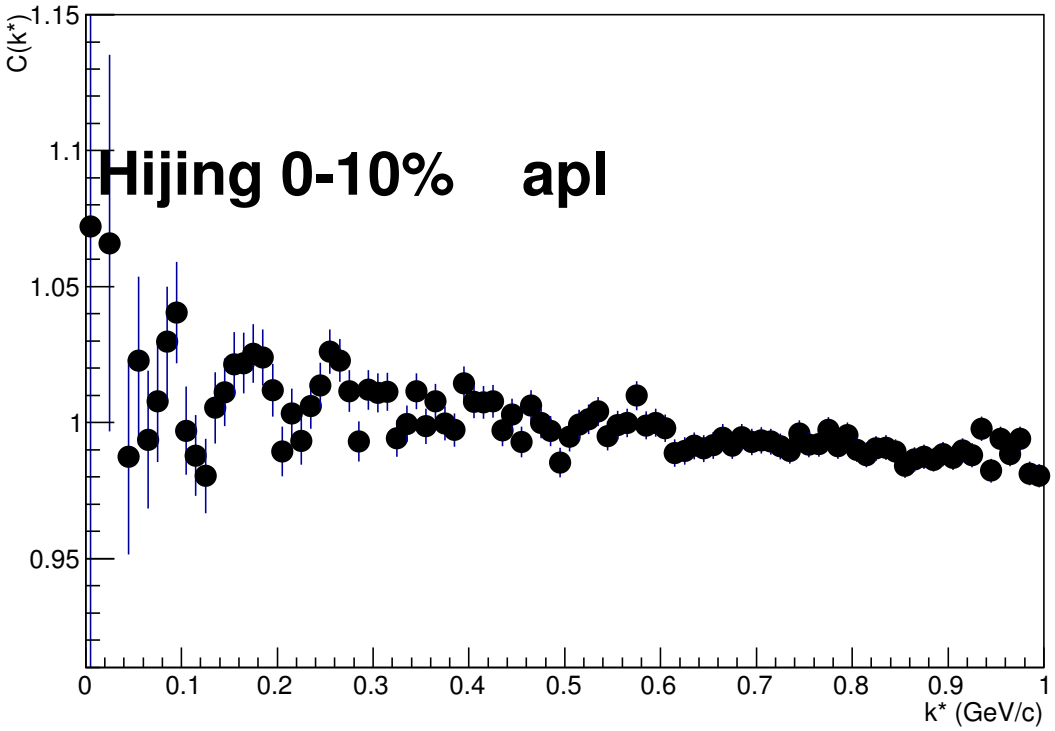

Fig. 17: $\bar{p}\Lambda$ correlation function, centrality 0-10%, hijing

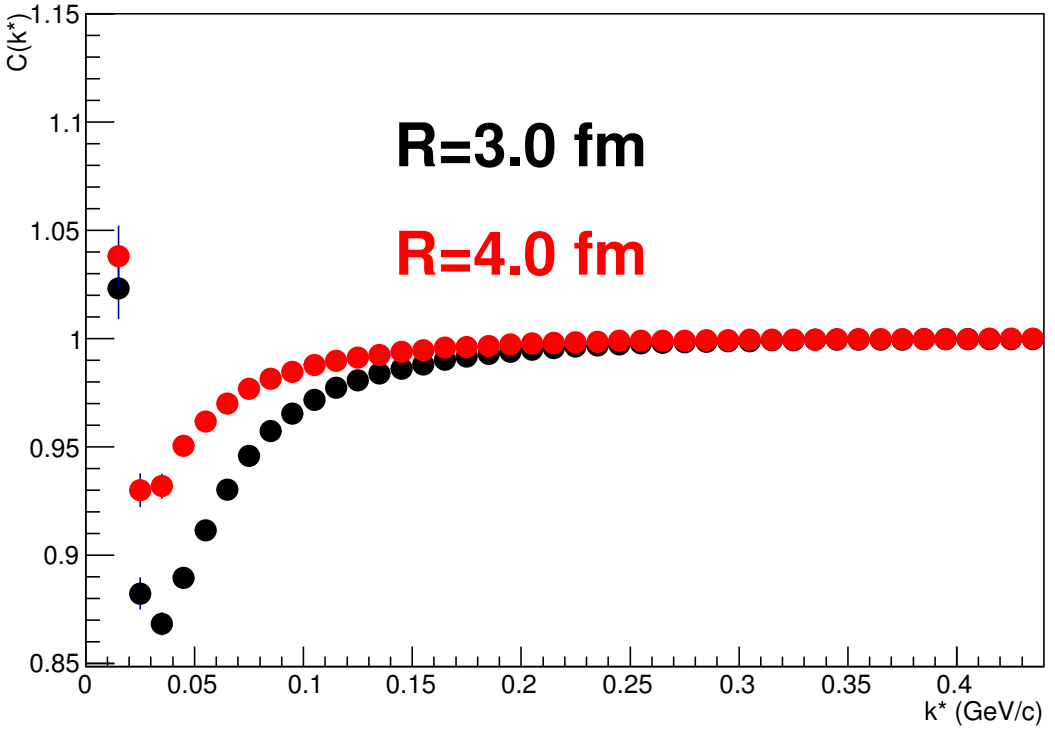

Fig. 18: $p\bar{p}$ correlation function generated using Lednicky's weights and assuming Gaussian source.

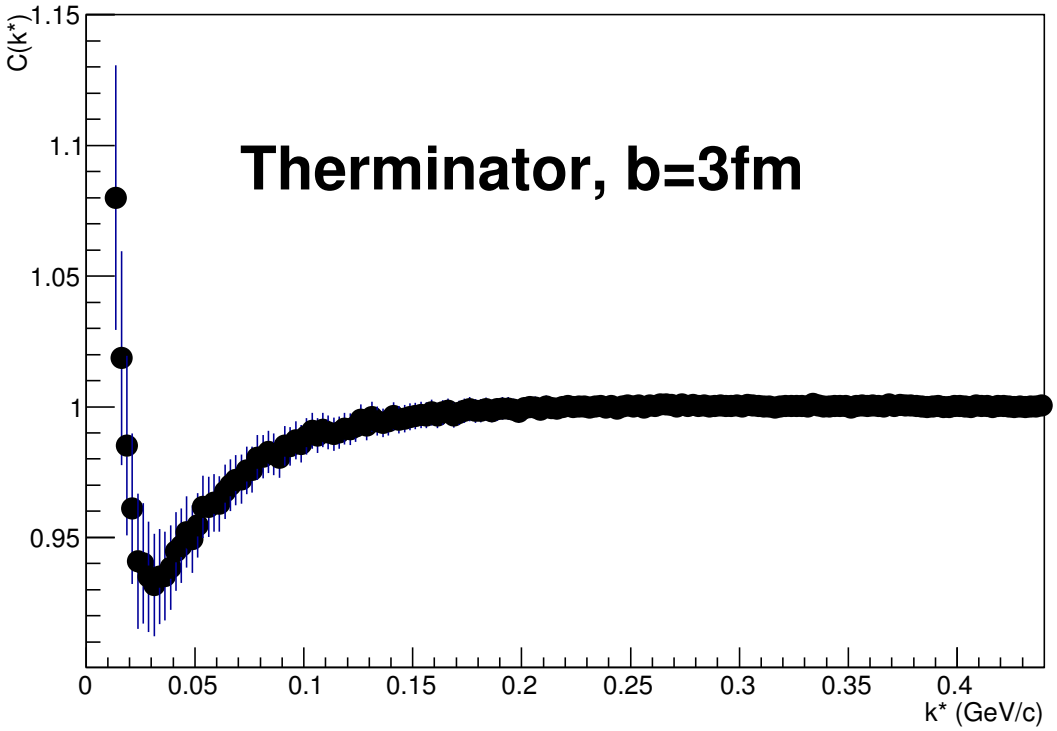

Fig. 19: $p\bar{p}$ correlation function generated using source from Therminator simulation and Lednicky's weights.

Gaussian source

Therminator source

3.2.3 $p\bar{\Lambda}$ *and* $\bar{p}\Lambda$ *theoretical function*

3.2.4 Fitting results

AQM

Simultaneous

Global

R fixed

f0 fixed

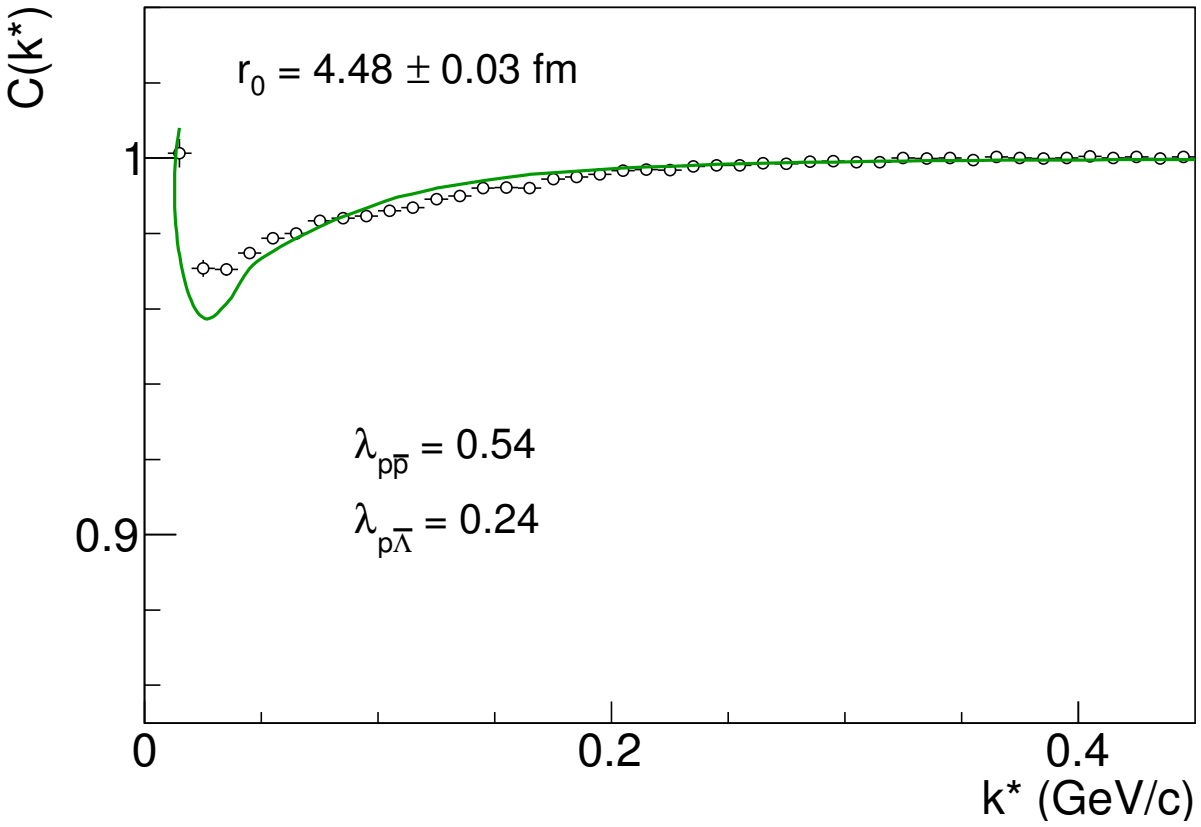

Fig. 20: Fit to p$\bar{\text{p}}$ correlation function divided by pol4, centrality 0-10%

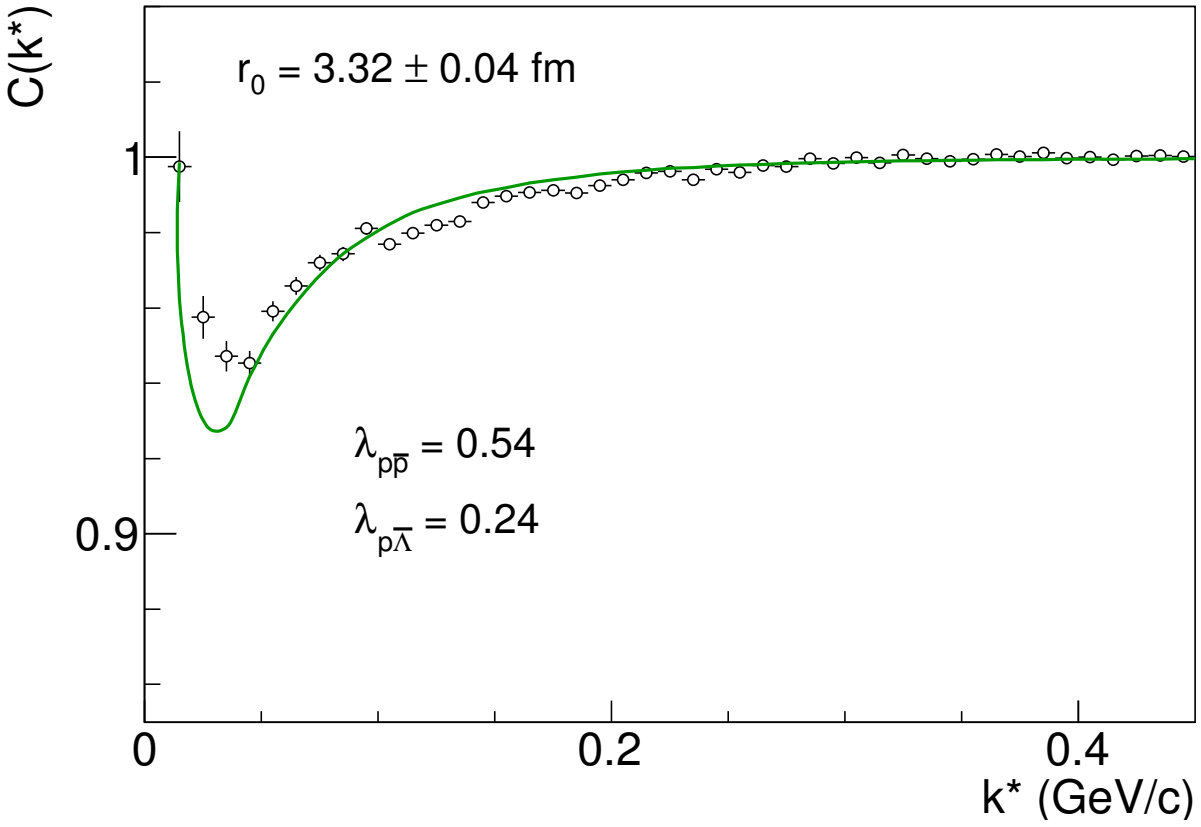

Fig. 21: Fit to p$\bar{\text{p}}$ correlation function divided by pol4, centrality 10-30%

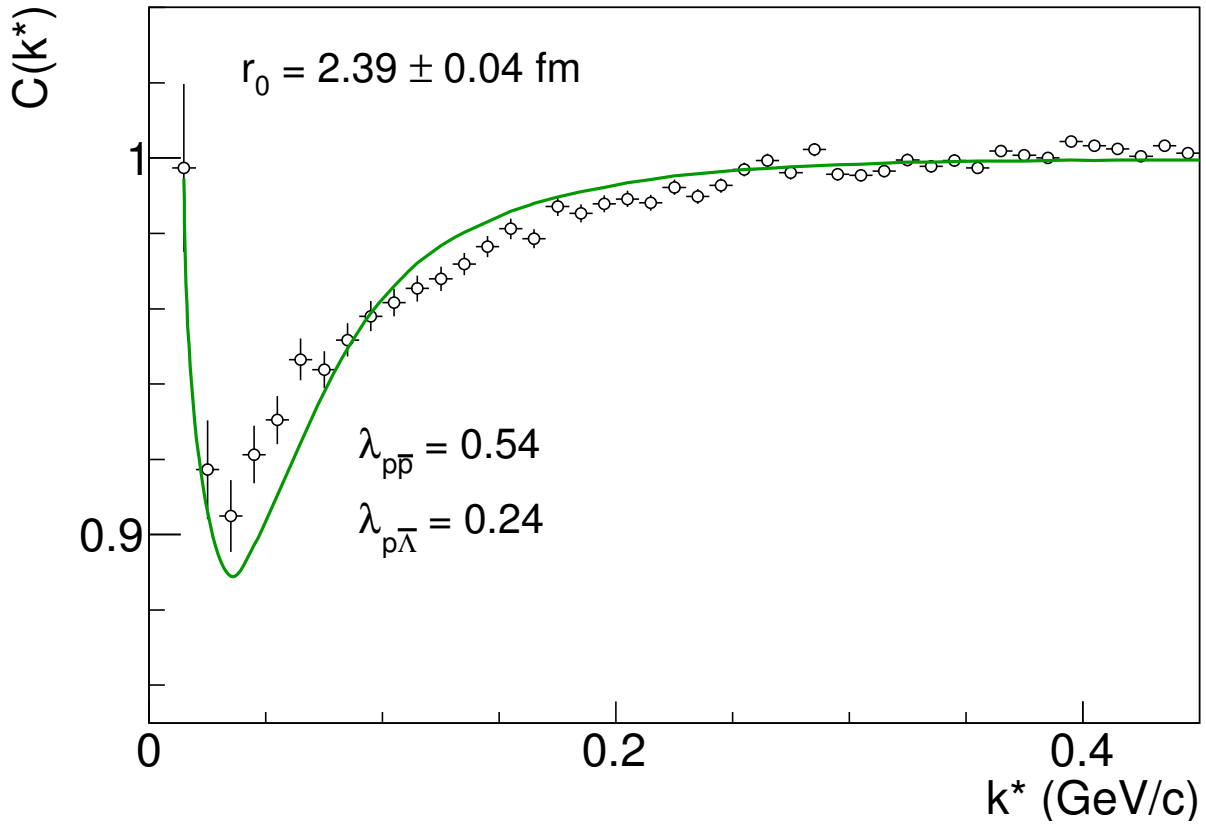

Fig. 22: Fit to p$\bar{\text{p}}$ correlation function divided by pol4, centrality 30-50%

3.3 Systematic uncertainties

3.3.1 non-femtoscopic background

3.3.2 fractions (Hijing vs. Therminator)

3.3.3 number of secondaries from material

3.3.4 momentum resolution correction

3.3.5 ALICE magnetic fields ++ vs. - -

3.3.6 PID

3.3.7 different scenarios for interaction parameters

3.3.8 DCA templates

3.3.9 p$\bar{\Lambda}$ *vs.* $\bar{\text{p}}\Lambda$

3.3.10 fitting procedure

3.3.11 Momentum resolution

Correction for momentum resolution is taken into account in the fitting procedure. Fit function is smeared with a gaussian function with the width corresponding the momentum resolution for the pairs of interest. Following formula is used:

$$C_c(q_c) = \int_{-3\sigma}^{+3\sigma} C_{th}(q_c - q) Gaus(q_t, \sigma)(q) |q_c - q|^2 dq, \quad (1)$$

where C_c is the corrected function, C_{th} is the ideal function, σ is the momentum resolution.

References

[1] A. Kisiel, H. Zbroszczyk, and M. Szymanski, "Extracting baryon-antibaryon strong interaction potentials from p$\bar{\Lambda}$ femtoscopic correlation function", *Phys. Rev.* **C89** (2014) 054916, arXiv:1403.0433 [nucl-th].